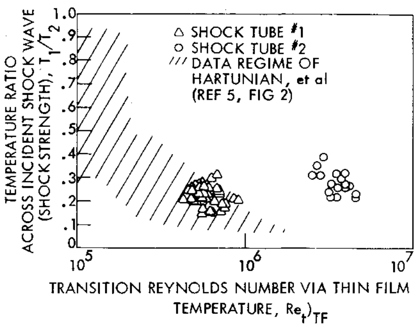

Fig. 3 Comparison of transition data with previous literature.

It is important to emphasize that this bias occurs regardless of the magnitude of the random error. When the random error is relatively large the bias tends to be obscured. But when the random error is relatively small the bias becomes evident and emphasizes the need for care in selection of instrumentation and data reduction procedures.

Schlieren Comparison

Figure 2 is a comparison of transition times obtained from schlieren photographs with those obtained simultaneously from thin-film recordings. This figure reveals the schlieren technique to generally yield lower transition times than the thin-film recordings for the same experimental run. In this case the bias plus random error (data scatter) is a maximum of about 50%. The least square line fitting this data has a slope of 0.84 ± 0.06 with 95% confidence. Thus, the bias is about 16% in this case. The additional scatter in the data is caused by difficulty in reading or determining transition from the schlieren photographs.

Comparison with Previous Literature

Figure 3 is a comparison of the thin-film transition data from these experiments with a summary of earlier transition data presented by Harturian, Russo, and Marrone.[5] The cross-hatched portion of Fig. 3 shows both the range and scatter of the data presented in Ref. 5. Different symbols are used to represent the data from each shock-tube facility used in these experiments. Figure 3 shows good agreement of transition data through transition Reynolds numbers of 10^6.

An apparent transition reversal is noted in Fig. 3 where, from shock tube No. 2, at a lower freestream temperature (smaller heat flux to the wall) the transition Reynolds numbers are extended to above values available for comparison with existing literature as well as those obtained in shock tube No. 1. This effect is well known to exist in conventional steady flow boundary layers but has only been reported in the literature[8] for shock induced boundary layers where heat flux has been incident on the boundary layer from combustion reactions occurring in the mainstream. Some difference in transition Reynolds number from each shock tube should be expected between these facilities because of uncontrolled factors in these experiments such as freestream turbulence, surface roughness, three-dimensional effects, and shock tube size.[3,9] Even though these differences are not quantified in these experiments the data from shock tube No. 1 compares well with the data of Ref. 5 which was obtained from a variety of facilities where, in some cases, the experimental conditions were carefully controlled. Thus, since the differences noted in Fig. 3 are larger than the possible uncertainties in the data, this reversal effect is believed to be real and is reported herein for your consideration.

References

[1] Mirels, H., "Laminar Boundary Layer Behind a Strong Shock Moving into Air," TN D-291, Feb. 1961, NASA.

[2] Wilson, R., "Viscosity and Heat Transfer Effects," *Handbook of Supersonic Aerodynamics*, Vol. 5, Sec. 13–14, U.S. Bureau of Naval Weapons NAVORD Rept. 1488, 1966.

[3] Davies, W. R. and Bernstein, L., "Heat Transfer and Transition to Turbulence in the Shock Induced Boundary Layer on a Semi-Infinite Flat Plate," *Journal of Fluid Mechanics*, Vol. 36, Pt. 1, March 1969, pp. 87–112.

[4] Bromberg, R., "Use of the Shock Tube Wall Boundary Layer in Heat Transfer Studies," *Jet Propulsion*, Vol. 26, Sept. 1956, pp. 737–740.

[5] Hartunian, R., Russo, A., and Marrone, P., "Boundary-Layer Transition and Heat Transfer in Shock Tubes," *Journal of the Aerospace Sciences*, Vol. 27, Aug. 1960, pp. 587–594.

[6] Henshall, B. and Schultz, D., "Some Notes on the Use of Resistance Thermometers for Measurement of Heat-Transfer Rates in Shock Tubes," Great Britain Aeronautical Research Council Current Paper 408, London, England, 1959.

[7] Taylor, B., "Development of a Thin Film Heat-Transfer Gauge For Shock Tube Flows," Technical Note 27, Institute of Aerophysics, University of Toronto, Toronto, Canada, 1959.

[8] Hall, J. L., Serovy, G. K., and Belles, F., "Effects of Heat Energy Release from Shock Induced Exothermic Reactions on Boundary Layer Transitions in Shock-Tube Flows," *Heat Transfer 1970*, Vol. III, Paper FC 9.2, Fourth International Heat Transfer Conference, Paris-Versailles, France, 1970.

[9] Braslow, A. L., "A Review of Factors Affecting Boundary-Layer Transition," TN D-3384, Aug. 1966, NASA.

Minimum Length Axisymmetric Laval Nozzles

LUCIAN Z. DUMITRESCU*
Institute of Fluid Mechanics and Aerospace Technology, Bucharest, Romania

I. Introduction

THIS paper deals with the determination of a class of minimum-length axisymmetric Laval nozzles, which are compared to the simple conical type, emphasizing the extra length needed to ensure uniform flow conditions. Submission of the paper has been prompted by the publication of Ref. 1; in fact, most of the following results have been obtained (and applied) over ten years ago, including the derivation of the hodograph equation for axisymmetric source flow, Eq. (4), but were left dormant in a journal of limited circulation.[2]

II. Basic Equations

Referring to Fig. 1, consider a spherical source flow, which is supersonic at distances r greater than the critical radius r_c. Writing that the mass flow m is constant at any distance:

$$4\pi r^2 \rho V = m = \text{const} \tag{1}$$

one obtains readily (see, e.g., Ref. 3, p. 372):

$$R^2 = (r/r_c)^2 = \frac{1}{M}\left(\frac{2}{\gamma+1} + M^2\right)^{(\gamma+1)/2(\gamma-1)} \tag{2}$$

Now, along a characteristic line BB' of this source flow, the velocity vector makes an angle $\mu = \text{arc sin}\,(1/M)$ with the local tangent. Therefore, one has:

$$r\,d\theta/dr = -tg\mu = -1/(M^2-1)^{1/2} \tag{3}$$

But the ratio dr/r may be obtained by differentiating Eq. (2). After integration of Eq. (3) the following fundamental formula results:

Received June 5, 1975.
Index categories: Nozzle and Channel Flow; Supersonic and Hypersonic Flow.
* Senior Scientist; Head, Shock-Tube Laboratory.

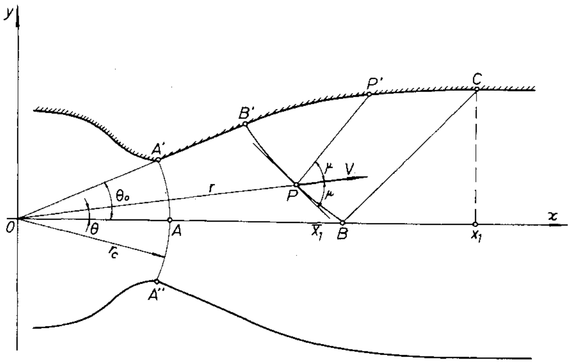

Fig. 1 Characteristic lines and nozzle contour.

$$\theta = \tfrac{1}{2}[\phi(M_1) - \phi(M)] \quad (4)$$

where $\phi(M)$ is the Prandtl-Meyer deviation angle for a plane supersonic flow of Mach number M (Ref. 3, p. 351):

$$\phi(M) = [(\gamma+1)/(\gamma-1)]^{1/2} \operatorname{arc} tg[(M^2-1)(\gamma-1)/(\gamma+1)]^{1/2} - \operatorname{arc} tg(M^2-1)^{1/2} \quad (5)$$

and M_1 is the reference Mach number at point B on the axis. Equation (4) [Eq. (20) of Ref. 2] is identical with Eq. (9) of Ref. 1 and shows that in the axisymmetric case, the flow deviation has half the two-dimensional value. Thus, existing tables for plane supersonic flow can be used.

III. Determination of the Nozzle Contour

From now on, the computation closely follows the method devised by Atkin[4] for plane nozzles (see also Ref. 3, p. 432). The nozzle is designed with an initial expansion angle θ_o (Fig. 1), the sonic surface being the spherical segment $A'AA''$. Formulas 2 and 4 represent the parametric equations of the line BB' in polar coordinates (r, θ), with M as parameter.

Now, if the flow at the downstream end of the nozzle is to be uniform, the characteristic line BC must be straight, and so must also be all characteristics PP' starting from points along BB'. To find the nozzle contour $B'C$, let m_1 be the mass flow through the conical surface generated by rotating the line PP' along the Ox axis:

$$m_1 = \pi\rho V[(r\sin\theta + lr\sin\mu)^2 - r^2\sin^2\theta] \quad (6)$$

where

$$l = \overline{PP'}/r \quad (7)$$

The value of m_1 has to be equated to the mass flow m_2 of the source, in the solid angle defined by the difference $\theta_o - \theta$:

$$m_2 = 2\pi\rho V r^2(\cos\theta - \cos\theta_o) \quad (8)$$

One obtains:

$$l = \{-\sin\theta + [\sin^2\theta + 2(\cos\theta - \cos\theta_o)]^{1/2}\}\sin\mu \quad (9)$$

and finally, the parametric equations of the contour $B'C$:

$$x/r_c = R[\cos\theta + l\cos(\mu+\theta)] \quad (10)$$

$$y/r_c = R[\sin\theta + l\sin(\mu+\theta)] \quad (11)$$

Here, R, θ, l, and μ are functions of the parameter M through Eqs. (2), (4), and (9). The constants to be specified are M_1, the nozzle Mach number, and θ_o, the initial expansion angle. The scaling length r_c may be related to the throat diameter, $d_o = 2r_c\sin\theta_o$, or to the mass flow m_o which has to pass through the nozzle (and to the stagnation gas parameters p_o, a_o):

$$r_c^2 = \frac{m_o}{2\pi}\frac{a_o}{\gamma p_o}\frac{1}{1-\cos\theta_o}\left(\frac{\gamma+1}{2}\right)^{\gamma+1/2(\gamma-1)} \quad (12)$$

The contour $B'C$ is obtained by giving values to the parameter M in the range $M_o < M < M_1$.

The value of M_o, which corresponds to point B' is implicitly determined from the following equation:

$$\phi(M_o) = \phi(M_1) - 2\theta_o \quad (13)$$

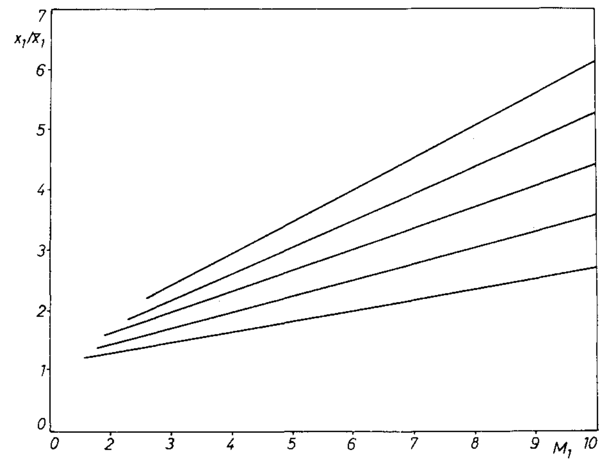

Fig. 2 Comparison of conical and profiled nozzle lengths, $2\theta_0 = 10°, 15°, 20°, 25°, 30°$.

A computer program producing the nozzle contour has been written and is available upon request. Boundary-layer corrections may readily be applied by standard methods.

IV. Discussion: Nozzle Length

It should be pointed out that this class of nozzles has the shortest length possible for uniform outflow, since the expansion starts with the maximum angle $2\theta_o$ from the throat. However, by comparison with a simple conical nozzle of same divergence angle, a considerable distance is needed to straighten the flow. If the nozzle length is considered as the distance from the throat to the apex of the test rhombus (point B), the two types of nozzles have equal lengths; however, the total lengths are in the ratio:

$$x_1/\bar{x}_1 = 1 + 2(M^2-1)^{1/2}\sin(\theta_o/2) \quad (14)$$

In Fig. 2, this ratio has been plotted for various expansion angles, as function of the Mach number M_1.

It is readily seen that, if a moderate divergence of the streamlines is acceptable, the simple conical nozzle is much shorter. This might be of considerable importance in some applications, e.g., gasdynamic lasers, where the fastest expansion rate possible of the gas is sought. Of course, the expansion angle $2\theta_o$, on which the length also depends, is limited by boundary-layer separation. Another feature of the forementioned class of nozzle is the condition at the throat: the assumption of a spherical sonic surface is closer to the real shape produced by the convergent part of the nozzle than the plane sonic surface usually considered for the design of plane or axisymmetric nozzles by other methods.

V. Experimental Results

A hypersonic shock tunnel[5] was equipped with a set of conical and contoured nozzles with an expansion angle $2\theta_o = 30°$ for $M_1 = 4, 7$, and 10. The Mach numbers measured in the straight and profiled nozzles coincided within the experimental errors and the tunnel has been in operation now for over ten years.

References

[1] Reddall, W. F. III, "Spherically-Symmetric Supersonic Source Flow: A New Use for the Prandtl-Meyer Function," *AIAA Journal*, Vol. 11, Dec. 1973, pp. 1787–1789.

[2] Dumitrescu, L. Z., "A Simple Analytical Method for the Design of Axisymmetric Laval Nozzles" (in Romanian), *Revista Transporturilor*, Bucharest, Vol. 10, Aug. 1963, pp. 355–359.

[3] Carafoli, E., "High-Speed Aerodynamics," Editura Tehnică, Bucharest, 1956.

[4] Atkin, A. O. L., "Two-Dimensional Supersonic Channel," *R and M 2174*, Pt. I, London, 1953.

[5] Dumitrescu, L. Z., "Studies in Shock Tubes" (in Romanian), Editura Academiei, Bucharest, 1969, pp. 147, 245–249.